Estimation of Gas-Phase Acidities of Deoxyribonucleosides: An Experimental and Theoretical Study

Sangeeta Kumari,[a] Chebrolu Lavanya Devi,[b] Sripadi Prabhakar,[a] Kotamarthi Bhanuprakash,[b] and Mariappanadar Vairamani[a]

[a] National Center for Mass Spectrometry, Indian Institute of Chemical Technology, Hyderabad 500 607, India
[b] Inorganic Chemistry Division, Indian Institute of Chemical Technology, Hyderabad 500 607, India

We determined the gas-phase acidities (ΔH_{acid}) of four deoxyribonucleosides, i.e., 2′-deoxyadenosine (dA), 2′-deoxyguanosine (dG), 2′-deoxycytidine (dC), and 2′-deoxythymidine (dT) by applying the extended kinetic method. The negatively charged proton-bound hetero-dimeric anions, $[A - H - B]^-$ of the deoxyribonucleosides (A) and reference compounds (B) were generated under electrospray ionization conditions. Collision-induced dissociation spectra of $[A - H - B]^-$ were recorded at four different collision energies using a triple quadrupole mass spectrometer. The abundance ratios of the individual monomeric product ions were used to determine the ΔH_{acid} of the deoxyribonucleosides. The obtained ΔH_{acid} value follows the order dA > dC > dT > dG. The ΔG_{acid} (298 K) values were determined by using $\Delta G_{acid} = \Delta H_{acid} - T\Delta S_{acid}$ where the ΔH_{acid} and ΔS_{acid} values were determined directly from the kinetic method plots. The ΔH_{acid} values were also predicted for the deoxyribonucleosides at the B3LYP/6-311+G**//B3LYP/6-311G** level of theory. The acidity trend obtained from the computational investigation shows good agreement with that obtained experimentally by the extended kinetic method. Theoretical calculations provided the most preferred deprotonation site as C5′-OH from sugar moiety in case of dA, and as $-NH_2$ (dC and dG) or −NH- (dT) from nitrogenous base moiety in the case of other deoxyribonucleosides. (J Am Soc Mass Spectrom 2010, 21, 136–143) © 2010 American Society for Mass Spectrometry

Deoxyribonucleosides are fundamental building blocks of DNA and play a major role in therapeutic applications as antiviral agents [1]. The determination of thermochemical properties of these molecules in the gas phase could be of importance for biological reasons because biological environment can be relatively nonpolar in nature. Moreover, the gas-phase studies explore the reactivity of molecules and ions without solvent effects. To date, mass spectral studies have been focused towards analysis and structural characterization of deoxyribonucleosides [2–10]. While thermochemical properties of individual nucleobases have been well studied experimentally in the gas phase, the studies on nucleosides are limited [11–16].

Xia et al. [11] performed extensive calculations on proton affinities (PAs) of nucleosides by the density functional approach. The PA of the four deoxyribonucleosides, i.e., 2′-deoxyadenosine (dA), 2′-deoxyguanosine (dG), 2′-deoxycytidine (dC), and 2′-deoxythymidine (dT) were reported to be in the order of dG > dC > dA > dT, and this order is similar to the PA order of the free bases (G > C > A > T). They concluded the protonation features of deoxyribonucleosides were less changed compared with the corresponding free bases. Donna et al. [12] determined the PA of dA and demonstrated the effective use of the kinetic method for the thermochemical measurement of multifunctional molecules like nucleosides and nucleobases. Besides the wide array of proton affinity studies on deoxyribonucleosides [13–16], there have been no experimental or theoretical reports on the gas-phase acidities (ΔH_{acid}) of deoxyribonucleosides. In this study, we report the first determination of ΔH_{acid} of dA, dG, dC, and dT through application of the extended kinetic method. We have also calculated the ΔH_{acid} values of the deoxyribonucleosides by applying theoretical calculations to investigate the influence of glycosyl group on the ΔH_{acid} of deoxyribonucleosides.

Computational

All calculations were carried out using the Gaussian 03w software [17]. Most stable structures of deoxyribonucleosides were taken from the earlier reports [18]. Geometrical optimizations and the vibrational frequencies of the neutral and deprotonated forms of all deoxyribonucleosides were carried out with B3LYP

Address reprint requests to Dr. M. Vairamani, National Center for Mass Spectrometry, Indian Institute of Chemical Technology, Hyderabad 500 607, India. E-mail: mvairamani@hotmail.com

1044-0305/10/$32.00
doi:10.1016/j.jasms.2009.09.019

Published online September 30, 2009
Received June 26, 2009
Revised September 22, 2009
Accepted September 23, 2009

method using 6-311G(d,p) basis set. Total electronic energies were obtained by single point calculations at the higher basis set 6-311+G(d,p). The zero-point vibrational energies and thermal corrections from the frequency analysis at the B3LYP/6-311G(d,p) level were considered to provide enthalpies at 298.15 K.

The gas-phase acidities were calculated using the following equation by directly taking enthalpy of proton as $\frac{5}{2}RT$ [19]

$$HA \rightarrow H^+ + A^- \quad (1)$$

$$\Delta_{acid}H^0_{298} = H^0_{298}(A^-) - H^0_{298}(AH) + \frac{5}{2}RT \quad (2)$$

Experimental

Materials

All the chemicals were procured from Aldrich (Steinheim, Germany) and were used without further purification. Stock (1 mM) solutions of the deoxyribonucleosides and the references (listed in Table 1) were prepared in basic (1% NH_4OH) methanol:water solution (50:50, vol:vol). The stock solutions of the deoxyribonucleosides and the references were mixed in appropriate volumes and diluted with methanol to achieve a final concentration of 50 μM each. Sample solutions were introduced into the source of the mass spectrometer by using inbuilt syringe pump at a flow rate of 5 μL/min.

Mass Spectrometry

Experiments were performed using a Quattro micro LC triple-quadrupole mass spectrometer (Waters, Manchester, UK) interfaced to an ESI source; data acquisition was done under the control of MassLynx software (version 4.1). Typical settings were capillary voltage −2.5 to −3 kV, cone voltage 10–15 V, source temperature 100 °C, desolvation temperature 100 °C. Nitrogen was used as desolvation and nebulization gas. The CID spectra were obtained by selecting the proton-bound hetero-dimeric anions with the first quadrupole (MS1), fragmenting them in the collision cell at four different collision energies (5, 8, 10, and 12 eV) in the laboratory frame, and recording the resulted fragment ions by scanning the second quadrupole (MS^2). Argon was used as the collision gas at a pressure of 5.0×10^{-4} mbar. Under the experimental conditions the number of collisions with the target may be 3–10 [20].

The Kinetic Method

The kinetic method developed by Cooks and coworkers [21, 22] is widely applied in gas-phase thermochemical measurements. In this method, proton-bound heterodimeric anions between molecule of interest (A) and a set of reference acids (B) are generated. These ions are subjected to collision induced dissociation (CID), which results into individual monomeric anions through competitive dissociations (eq 3).

$$[A] + [B - H]^- \overset{k_2}{\leftarrow} [A - H - B]^- \overset{k_1}{\rightarrow} [A - H]^- + [B] \quad (3)$$

The abundance ratio $[A - H]^-/[B - H]^-$ reflects the rate constant ratio k_1/k_2,where k_1 and k_2 are the rate constants for the competitive dissociations of the dimeric anion to produce $[A - H]^-$ and $[B - H]^-$, respectively. The ratio of rate constants can be derived using unimolecular reaction theory (eq 4) [21, 22].

$$\ln [A - H^-/B - H^-] = \Delta(\Delta S)/R + \Delta H_{acid}(A)/RT_{eff} - \Delta H_{acid}(B)/RT_{eff} \quad (4)$$

Table 1. Reference compounds used and their ΔG, ΔH and ΔS values[a]

Analyte	Reference	ΔG (kJ/mol)	ΔH (kJ/mol)	ΔS (J/mol)
2′-Deoxy-guanosine	3-Nitro-benzoic acid	1347 ± 8.4	1377 ± 8.8	100.6
	4-Hydroxy-benzaldehyde	1364 ± 8.4	1393 ± 8.8	97.3
	3-Nitrophenol	1370 ± 8.4	1399 ± 8.8	97.3
	4-Hydroxy-acetophenone	1375 ± 8.4	1404 ± 8.8	97.3
2′-Deoxy-thymidine	3-Hydroxy-benzoic acid	1387 ± 8.4	1417 ± 8.8	100.6
	Benzoic acid	1394 ± 8.4	1423 ± 9.2	97.3
	4-methyl-benzoic acid	1396 ± 8.4	1425 ± 8.8	97.3
	3-Amino-benzoic acid	1400 ± 8.4	1429 ± 8.8	97.3
2′-Deoxy-cytidine	3-Amino-benzoic acid	1400 ± 8.4	1429 ± 8.8	97.3
	3-Hydroxy-acetophenone	1404 ± 8.4	1433 ± 8.8	97.3
	4-Chloro-phenol	1407 ± 8.4	1436 ± 8.8	97.3
	2-*tert*-Butyl-phenol	1415 ± 8.4	1447 ± 9.2	107.3
2′-Deoxy-adenosine	2-*tert*-Butyl-phenol	1415 ± 8.4	1447 ± 9.2	107.3
	Resorcinol	1422 ± 8.4	1451 ± 8.8	97.3
	3-Cresol	1434 ± 8.4	1463 ± 8.8	97.3
	Hydroquinone	1436 ± 8.4	1466 ± 8.8	100.6

[a]ΔG and ΔH obtained from the NIST Chemistry Web book [27] and ΔS calculated from the equation ΔG = ΔH-TΔS at 298K.

With the first assumption that no reverse energy barrier exists for the two dissociation pathways (eq 3), and equal detection efficiencies for the two ions, the ratio $[A - H^-/B - H^-]$ is equal to the rate constant ratio (k_1/k_2). With the second assumption that both analyte and the reference bases are structurally similar and $\Delta(\Delta S) \approx 0$, the eq 4 can be rewritten as eq 5.

$$\ln (A - H^-/B - H^-) = \Delta H_{acid}(A)/RT_{eff} - \Delta H_{acid}(B)/RT_{eff} \quad (5)$$

This simple form of the kinetic method is applicable to most of the compounds assuming (1) the activation energies for reverse reactions are negligible, and (2i) entropy changes for the two fragmentation channels are the same. The first assumption is applied to weakly bound singly charged cluster ions, while the second assumption is valid only for the species without internal hydrogen bonding [21, 22].

If the reference compounds are structurally different from the analyte of interest, the eq 5 yields errors in the ΔH_{acid} values due to different entropic contributions between the two dissociation channels. In such cases, the extended kinetic method is used [23–30], where experiments are performed at different collision energies to measure variations in effective temperature T_{eff}. The plots of $\ln [A - H^-/B - H^-]$ measured at different collision energy versus the gas-phase acidities of the reference acids give a set of slopes and intercepts. When these slopes and intercepts are plotted against each other, it separates the entropy and enthalpy terms. The new regression line thus obtained gives ΔH_{acid} from the slope and $\Delta(\Delta S)$ from the intercept in accord with the relation shown in eq 6. The term in the square bracket represents an apparent $\Delta G_{acid}/RT_{eff}$ of the unknown acid A, where ΔG_{acid} defined by eq 7.

$$\ln\frac{k_1}{k_2} = \left[\frac{\Delta H_{acid}(A)}{RT_{eff}} - \frac{\Delta(\Delta S)}{R}\right] - \frac{\Delta H_{acid}(B)}{RT_{eff}} \quad (6)$$

$$\Delta G^{app}(A) = \Delta H_{acid}(A) - T_{eff}\Delta(\Delta S) \quad (7)$$

The term $\Delta(\Delta S)$ represents the difference in the entropy change for the two dissociation channels of the dimeric anion. Nevertheless, the new regression lines obtained from such data show almost perfect correlation coefficients that may lead to underestimated experimental uncertainties. To decrease the severity of this problem, Armentrout [30] suggested plotting $\ln [A - H^-/B - H^-]$ against $[\Delta H_{acid}(B) - \Delta H_{acid}(B_{avg})]$, where $\Delta H_{acid}(B_{avg})$ is the average gas-phase acidity value of all the references used for the particular measurement (statistical approach). The slope and intercept of this plot give $[1/RT_{eff}]$ and $\{-[\Delta H_{acid}(A) - \Delta H_{acid}(B)_{avg}]/RT_{eff} - (\Delta S)/R\}$, respectively. The plot of negative of intercepts against corresponding slopes, give $[\Delta H_{acid}(A) - \Delta H_{acid}(B)_{avg}]$ from the slope and $-\Delta(\Delta S)/R$ from the intercept. This method is used in cases where reference compounds are structurally different from the analyte of interest.

Results and Discussion

The structures of the studied deoxyribonucleosides (dA, dG, dC, and dT) are shown in Scheme 1. CID experiments were carried out on $[M - H - X]^-$, where ($X^- = Br^-, I^-, F^-, Cl^-, CH_3COO^-, CF_3COO^-, HCOO^-$) to evaluate the approximate ΔH_{acid} values and the relative acidities of the deoxyribonucleosides. When $X = F^-$ and CH_3COO^-, the spectra showed only $[M - H]^-$ ions and this suggests higher ΔH_{acid} values for the anions than that for the deoxyribonucleosides. In the case of Br^-, I^-, and CF_3COO^-, the spectra exclusively yielded X^- ion confirming lesser ΔH_{acid} for these anions than that for the deoxyribonucleosides. In the case of Cl^- and $HCOO^-$, the spectra showed both X^- and $[M - H]^-$ anions, and this shows that the ΔH_{acid} values of the deoxyribonucleosides studied are closer to that of Cl^- (ΔH = 1395 kJ/mol) and $HCOO^-$ anion (ΔH = 1444 kJ/mol) [31]. The CID spectra obtained with $HCOO^-$ (Figure 1) provides the relative acidity order for the deoxyribonucleosides as dA > dC > dT > dG.

With a view to determining the ΔH_{acid} values of deoxyribonucleosides (A) by applying the kinetic method, derivatives of aromatic compounds (mostly benzoic acid and phenol derivatives) were selected as the references (B). Four references were used for each deoxyribonucleoside, and their ΔG_{acid}, ΔS_{acid}, and ΔH_{acid} values are listed in Table 1 [32]. The CID spectra of the proton-bound hetero-dimeric anions $[A - H - B]^-$ were recorded at four collision energies: 5, 8, 10, and 12 eV. The spectra exclusively yielded two individual monomeric anions, $[A - H]^-$ and $[B - H]^-$ and ion abundances of these ions were used for the kinetic method process.

At first, the simple kinetic method was applied as described above (eq 5); $\ln [A - H]^-/[B - H]^-$ values were plotted against the ΔG_{acid} values of the reference compounds at 298 K. These plots resulted in a straight line with a slope $1/RT_{eff}$ and intercept $-\Delta G_{acid}/RT_{eff}$. The ΔG_{acid} values of deoxyribonucleosides were calcu-

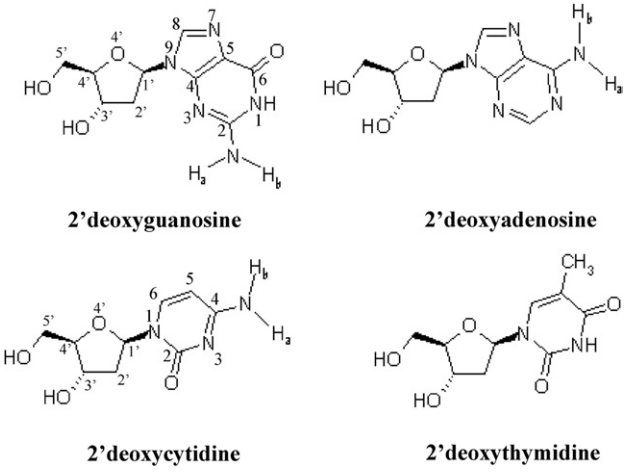

Scheme 1. Structures of deoxyribonucleosides with each atom numbered typically for purine and pyrimidine.

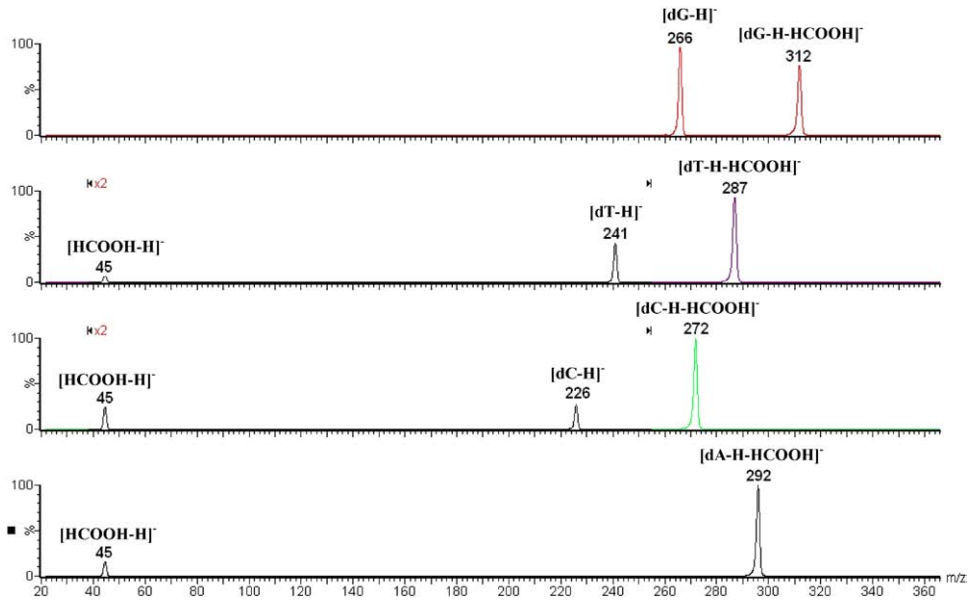

Figure 1. CID spectra of proton bound deprotonated deoxyribonucleosides and formate anion at constant collision activation conditions.

lated from the slopes and intercepts (data presented in Table S1 of Supplementary Material, which can be found in the electronic version of this article). Among the deoxyribonucleosides, dA has the highest ΔG_{acid} and dG the lowest. However, it was noticed that upon collision energy increase there was a small but significant change in the ΔG_{acid} values ranging from 1 to 3 kJ/mol (shown in Table S1 of Supplementary Material), which could be due to the entropy effects. Thus, we applied the extended kinetic method suggested by Armentrout [30] to determine enthalpy differences.

The plots of ln $\{[A - H^-]/[B - H^-]\}$ obtained at each specific collision energy against $[\Delta H_{acid}(B) - \Delta H_{acid}(B_{avg})]$ gave a straight line with slope $[1/RT_{eff}]$ and intercept $\{-[\Delta G^{app}(A) - \Delta H_{acid}(B)_{avg}]/RT_{eff}\}$. Such plots were attained at the four different collision energies; typical plots of dG are shown in Figure 2 (the plots of dA, dC, and dT are shown in Supplementary Material). Using the resultant slopes and intercepts, T_{eff} and $\Delta G_{acid}{}^{app}$ values

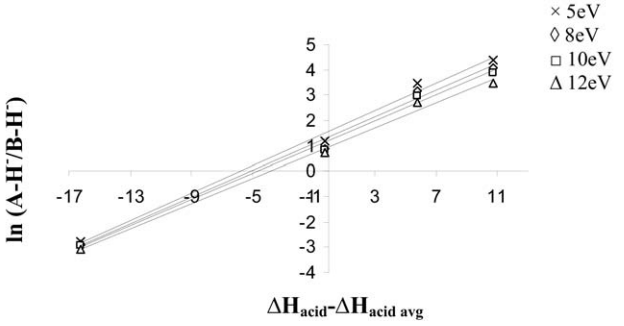

Figure 2. Plots of the measured product ion abundance ratio, ln $(A - H^-/B - H^-)$ for 2′-deoxyguanosine versus $\Delta H_{acid} - \Delta H_{acid\ avg}$ (kJ/mol) of reference compounds at 5, 8, 10, and 12 eV collision energy.

were obtained as tabulated in Table 2. To obtain the entropy term, the negatives of intercept obtained at different collision energies were plotted against the corresponding slopes (the plot of dG shown in Figure 3 as an example, and plots of dA, dC, and dT are shown in Supplementary Material). From this plot, the value of $[\Delta H_{acid}(A) - \Delta H_{acid}(B)_{avg}]$ and $[-\Delta(\Delta S_{acid})/R]$ were then extracted from the slope and the intercept, respectively.

The $\Delta G_{acid}{}^{app}$ and T_{eff} values increased as a function of collision energy (Table 2), signifying increased energy deposition with an increase in the collision energy. The ΔS_{acid} value of the analyte was calculated from the average value of ΔS_{acid} for the reference compounds at 298 K and the $\Delta(\Delta S_{acid})$ value obtained from the intercept of the plot (Table 2). These ΔS_{acid} values were used to calculate the ΔG_{acid} of the deoxyribonucleosides at 298 K, and are summarized in Table 2. The order of ΔH_{acid} values of deoxyribonucleosides determined from the extended kinetic method is found to be similar to the order of ΔG_{acid} values, mainly because of closer entropic contributions (Table 2) of deoxyribonucleosides.

The determined ΔH_{acid} values of the deoxyribonucleosides are in the order of dA > dC > dT > dG. Though the deoxyribonucleosides dA and dG come under the purine base containing deoxyribonucleosides, a large difference exists between their ΔH_{acid} values. The measured ΔH_{acid} values for dA and dG are in good agreement with their known solution phase acidity constant values in the literature. The deoxyribonucleosides dA and dG were well studied in the solution phase because of their self-association properties (stacking interactions) [33–35]. The acidity constant values obtained for dG and dA from potentiometric pH titrations in dilute aqueous solutions [35] were 2.30 and

Table 2. The ΔH, ΔS, and ΔG values for deoxyribonucleosides obtained by the extended kinetic method*

Comp.	ΔG^{app} (kJ/mol) 5 eV	8 eV	10 eV	12 eV	ΔH_{acid} (kJ/mol)	ΔS (J/mol/k)	ΔG_{acid} = ΔH-TΔS (kJ/mol)
							at 298 K
dG	1387.4 ± 0.1 [465]	1388 ± 0.1 [477]	1388.6 ± 0.1 [489]	1389.2 ± 0.1 [507]	1367 ± 2.2 (5.4)	53.7 ± 3.8	1351 ± 1.0 (2.4)
dA	1462 ± 0.1 [662]	1464.3 ± 0.1 [702]	1466 ± 0.1 [746]	1467.3 ± 0.2 [772]	1430 ± 1.5 (3.7)	52.5 ± 2.7	1415 ± 0.7 (1.7)
dC	1455.8 ± 0.2 [530.5]	1457.2 ± 0.1 [545]	1458.3 ± 0.0.1 [571]	1459.6 ± 0.2 [601]	1409 ± 2.5 (6.0)	47.0 ± 4.4	1394.6 ± 1.2 (2.9)
dT	1428.6 ± 0.0.7 [563]	1430.4 ± 0.1.0 [594]	1431.4 ± 0.0.9 [611]	1432.8 ± 1.0 [640]	1399 ± 1.7 (4.0)	42.8 ± 3.4	1386 ± 1.0 (2.4)

*The value in the [ ] indicates T_{eff} values in K. ± Standard deviation from the triplicate data. The value in parentheses ( ) indicates uncertainties at 95% confidence limit.

3.74 (25 °C; I = 0.1M, $NaNO_3$), respectively. Higher the acidity constant value lower will be the acidity, and thus dG is more acidic than dA in aqueous solutions, and this correlates with the gas-phase results in the present study. The large difference in the measured ΔH_{acid} values of dA and dG could be due to structural differences in the nucleobases (adenine and guanine), because in both cases the bases are linked to the same sugar moiety at N-9 of the nucleobase through the glycosidic bond. The adenine and guanine have similar core structures but from the chemical point of view, these two bases differ significantly. Adenine has the primary amine group at C-6, whereas the guanine, in addition to the primary amine group at C-2, has an extra acidic proton at the N-1 that is in conjugation with the keto-group at C-6. These addition structural features in dG might be responsible for its least ΔH_{acid} value among the studied deoxyribonucleosides. Further, theoretical calculations were carried out for better understanding the experimentally obtained ΔH_{acid} order for deoxyribonucleosides.

Computational Results

Density functional theory (DFT) methods were used to study the ΔH_{acid} values of the deoxyribonucleosides. Topol et al. [36] calculated the ΔH_{acid} values of glycine and alanine using a variety of high-level theoretical methods. There was a good agreement of high level calculations results with the measured values; thus, they concluded the DFT methods represent the best tools for obtaining ΔH_{acid} values for medium to large sized molecular systems. Ground state geometries for the studied deoxyribonucleosides were taken from the earlier study [18], in which C3′-endo/anticonformer for dC and C2′-endo/anti for the remaining deoxyribonucleosides were considered. The reoptimized geometries of the molecules obtained at the B3LYP/6-311G** level of theory were in good agreement with the earlier reported data [18]. Single point energy calculations at B3LYP/6-311+G** were then performed at the B3LYP/6-311G** geometries to obtain the final total electronic energies. The total electronic energies at the B3LYP/6-311+G** geometries were converted to enthalpies at 298 K using unscaled vibrational frequencies at the B3LYP/6-311G** geometries. The calculated values of electronic energies, thermal corrections, and enthalpies at 298 K are given in Table 3. Optimized geometries of the lowest-energy neutrals and most stable deprotonated forms of deoxyribonucleosides are provided in Figure 4.

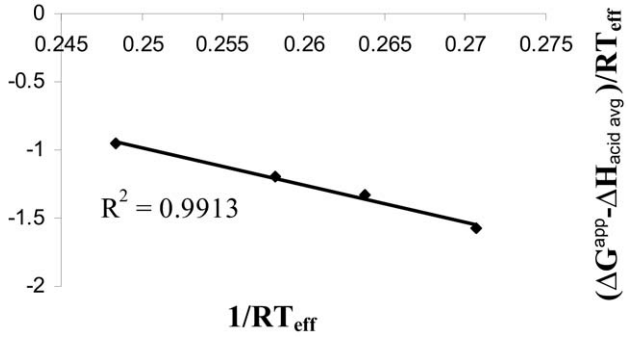

Figure 3. Plot of $\{(\Delta G^{app}(\mathbf{dG}) - \Delta H_{acid\ avg})/RT_{eff}\}$ versus $1/RT_{eff}$ used for 2′-deoxyguanosine to determine ΔH_{acid} from the slope and $\Delta\Delta S_{acid}$ from the intercept.

In the case of deoxyribonucleosides, the most acidic site of the free bases was substituted with sugar moiety. Therefore, the most acidic site in the deoxyribonucleosides can be presumed to be the second most acidic proton of the corresponding free nucleobase. Kenttamaa et al. [19, 37] calculated the ΔH_{acid} values of free nucleobases at all sites, and the order of ΔH_{acid} value for second most acidic proton was 9H-adenine (N4-H_b) > keto cytosine (N4-H_b) > thymine (N3-H) > 9H-keto-guanine(N2-H_b). In the present study, we obtain the ΔH_{acid} of deoxyribonucleosides (at the most acidic site) in the order of dA (C5′-OH) > dC (C4-N4-H_b) > dT (N3-H) > dG (C2-N2-H_b). The most acidic site in the deoxyribonucleosides is indeed the second most acidic site in the corresponding free nucleobases (except dA). The acidity order of the deoxyribonucleosides matches that of the free bases (at second most acidic site); hence introduction of a sugar moiety to the nucleobase does not change the acidity

Table 3. Calculated total electronic energies, zero-point energies, thermal corrections, and enthalpies at 298 K and gas phase acidities (ΔH_{acid}) of deoxyribonucleosides and their deprotonated forms (energies in hartrees)

	E_{tot}[a]	ZPVE[b]	H°[c]	H^{o}_{298}	ΔH^{o}_{298} (kJ/mol)
dC	−816.178221	0.232779	0.247760	−815.697681	
dC-H(C4-N-H_b)	−815.607143	0.218857	0.233358	−815.15493	1409
dC-H(C4-N-H_a)	−815.616579	0.219340	0.233777	−815.16346	1431
dC-H(C3′-OH)	−815.602673	0.217722	0.231819	−815.15313	1436
dC-H(C5′-OH)	−815.608141	0.217412	0.231409	−815.15932	1420
dG	−963.837878	0.251063	0.267714	−963.31910	
dG-H(N1-H)	−963.290902	0.237545	0.254791	−962.798566	1373
dG-H (C2-N-H_b)	−963.285232	0.237202	0.253463	−962.794566	1365
dG-H(C2-N-H_a)	−963.293299	0.237656	0.253874	−962.801769	1383
dG-H(C3′-OH)	−963.255873	0.235261	0.251727	−962.768885	1451
dG-H(C5′-OH)	−963.263161	0.235692	0.251587	−962.775881	1432
dT	−875.399654	0.249067	0.265225	−874.885362	
dT-H(N3-H)	−874.840665	0.234475	0.250416	−874.355773	1398
dT-H1(C3′-OH)	−874.819491	0.233004	0.248998	−874.337072	1446
dT-H2(C5′-OH)	−874.83418	0.233563	0.248929	−874.351687	1407
dA	−888.576763	0.246188	0.261900	−888.068675	
dA-H(C6-N-H_b)	−888.002181	0.232526	0.247710	−887.521944	1439
dA-H(C6-N-H_a)	−888.003191	0.232431	0.247629	−887.523131	1442
dA-H(C3′-OH)	−887.993585	0.230578	0.245914	−887.517092	1454
dA-H(C5′-OH)	−888.004825	0.231030	0.245794	−887.528001	1426

[a]Single point energy calculation on at B3LYP/6-311+G(d,p) and optimized geometries at B3LYP/6-311G(d,p) [B3LYP/6-311+G(d,p)//B3LYP/6-311G(d,p)].
[b]Zero point vibrational energy at B3LYP/6-311G(d,p).
[c]Thermal correction at B3LYP/6-311G(d,p).

order. Thus, the deprotonation features of deoxyribonucleosides (except dA) are less changed than their corresponding bases [19, 37].

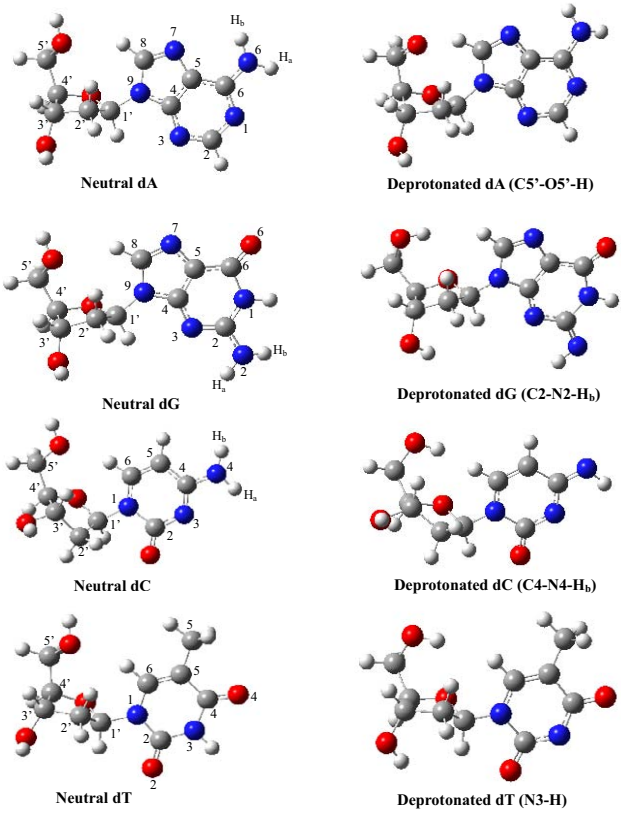

Figure 4. Geometries of neutral and most stable deprotonated forms of all the deoxyribonucleosides studied in this work.

In all nucleosides, with the exception of dA, the most acidic proton is available on the base moiety (Table 3). The presence of a keto group on the base moiety accommodates negative charge and forms a stable delocalized structure. Such a kind of keto group is absent in the nucleobase of dA, and loss of a proton from the NH_2 of the nitrogenous base moiety results in a double-bond character to the C6–N6 bond (1.29 A^0). This leads to loss of resonance in the purine ring, hence deprotonation from nucleobase is unfavorable in dA. Between the two possible deprotonation sites (C3′-O3′-H and C5′-O5′-H) of the sugar moiety, C5′-O5′-H is the most favored deprotonation site in dA. The computational evaluation of ΔH_{acid} values of deoxyribonucleosides is in good agreement with the experimental results within the deviation ranges <5 kJ, (Table 4) and found to be in the order dA > dC > dT > dG. Further information regarding the optimized structures of the studied deprotonated forms of all nucleosides are provided in the Supplementary Materials (Figure S7–S10).

Table 4. Experimental and theoretical gas phase acidity (ΔH_{acid}) values (kJ/mol) of studied deoxyribonucleosides*

Deoxyribonucleosides	ΔH_{298K} (theoretical)	ΔH (experimental)
2′-Deoxyguanosine	1365	1367 ± 2.2 (5.4)
2′-Deoxythymidine	1398	1399 ± 1.7 (4.0)
2′-Deoxycytidine	1409	1409 ± 2.5 (6.0)
2′-Deoxyadenosine	1426	1430 ± 1.5 (3.7)

*Standard deviation from the triplicate data. The value in parentheses ( ) indicates uncertainties at 95% confidence limit.

Conclusion

Here we report ΔH_{acid} values of four deoxyribonucleosides (dA, dC, dG, and dT) for the first time measured by the extended kinetic method. Proton-bound heterodimeric anions of deoxyribonucleosides and a suitable reference acid were generated under negative electrospray ionization conditions, and dissociated appropriately in the collision cell. The relative abundances of the two monomeric product anions were used to measure the ΔH_{acid} values. The experiments performed at different collision energy values, and the ΔH_{acid} values were obtained by applying the extended kinetic method. The ΔH_{acid} values were also predicted computationally by using density functional methods at B3LYP/6-311+G**//B3LYP/6-311G** level of theory. The calculations revealed that the deprotonation is preferred from nitrogenous base, but in the case of dA, it is from the sugar moiety. The most favored deprotonation sites are C5′-OH of dA, C4-N4-H_b of dC, N3-H of dT, C2-N2-H_b of dG. The theoretical ΔH_{acid} values are in good agreement with the acidities obtained from the experiments by applying the extended kinetic method, and they are in order of dA > dC > dT > dG.

Acknowledgments

The authors thank Dr. J. S. Yadav, director of the Indian Institute of Chemical Technology, for the facilities and encouragement. S. K. and C. L. D. thank the Council of Scientific and Industrial Research, New Delhi, for the senior research fellowship.

Appendix A Supplementary Material

Supplementary material associated with this article may be found in the online version at doi:10.1016/j.jasms.2009.09.019.

References

1. Puech, F. A.; Pompon, I.; Lefebvre, G.; Gosselin, G.; Imbach, J. L. Nucleotidic Prodrugs of Anti-HIV Dideoxynucleosides. *Bioorg. Med. Chem. Lett.* **1992,** *2,* 603–606.
2. Biemann, K.; McCloskey, J. Application of Mass Spectrometry to Structure Problems. VI. Nucleosides *J. Am. Chem. Soc.* **1962,** *84,* 2005–2007.
3. Sakurai, T.; Matsuo, T.; Kusai, A.; Nojima, K. Collisionally Activated Decomposition Spectra of Normal Nucleosides and Nucleotides Using a Four-Sector Tandem Mass Spectrometer. *Rapid Commun. Mass Spectrom.* **1989,** *3,* 212–216.
4. Reddy, D.; Iden, C. R. Analysis of Modified Deoxynucleosides by Electrospray Ionization Mass Spectrometry. *Nucleosides Nucleotides.* **1993,** *12,* 815–826.
5. Hua, Y.; Wainhaus, S. B.; Yang, Y.; Shen, L.; Xiong, Y.; Xu, X.; Zhang, F.; Bolton, J. L.; van Breemen, R. B. Comparison of Negative and Positive Ion Electrospray Tandem Mass Spectrometry for the Liquid Chromatography Tandem Mass Spectrometry Analysis of Oxidized Deoxynucleosides. *J. Am. Soc. Mass Spectrom.* **2001,** *12,* 80–87.
6. Zhang, Q.; Wang, Y. Differentiation of 2′O- and 3′O-Methylated Ribonucleosides by Tandem Mass Spectrometry. *J. Am. Soc. Mass Spectrom.* **2006,** *17,* 1096–1099.
7. Kamel, A. K.; Munson, B. Collision-Induced Dissociation of Purine Antiviral Agents: Mechanisms of Ion Formation Using Gas-Phase Hydrogen/Deuterium Exchange and Electrospray Ionization Tandem Mass Spectrometry. *Eur. J. Mass Spectrom.* **2004,** *10,* 239–257.
8. Claereboudt, J.; Esmans, E. L.; Claeys, M. Mass Spectral Behavior of $(M - H)^-$ Ions of Some Pyrimidine Nucleosides. *Biol. Mass.Spectrom.* **1993,** *22,* 419–421.
9. Smith, D. L.; Schram, K. H.; McCloskey, J. A. The Negative Ion Mass Spectra of Selected Nucleosides. *Biomed. Mass Spectrom.* **1983,** *10,* 269–275.
10. Crow, F. W.; Tomer, K. B.; Gross, M. L.; McCloskey, J. A.; Bergstrom, D. E. Fast Atom Bombardment Combined with Tandem Mass Spectrometry for the Determination of Nucleosides. *Anal. Biochem.* **1984,** *139,* 243–262.
11. Xia, F.; Xie, H.; Cao, Z. Density Functional Study of Protonation of Deoxynucleosides: Electrophilic Active Sites and Proton Affinities. *Int. J. Quantum. Chem.* **2008,** *108,* 57–65.
12. DiDonna, L.; Napoli, A.; Sindona, G.; Athanassopoulos, C. A Comprehensive Evaluation of the Kinetic Method Applied in the Determination of the Proton Affinity of the Nucleic Acid Molecules. *J. Am. Soc. Mass Spectrom.* **2004,** *15,* 1080–1086.
13. Greco, F.; Liguori, A.; Sindona, G.; Uccella, N. Gas-Phase Proton Affinity of Deoxyribonucleosides and Related Nucleobases by Fast Atom Bombardment Tandem Mass Spectrometry. *J. Am. Chem. Soc.* **1990,** *112,* 9092–9096.
14. Liguori, A.; Napoli, A.; Sindona, G. Survey of the Proton Affinities of Adenine, Cytosine, Thymine, and Uracil Dideoxyribonucleosides, Deoxyribonucleosides, and Ribonucleosides. *J. Mass Spectrom.* **2000,** *35,* 139–144.
15. Wilson, M. S.; McCloskey, J. A. Chemical Ionization Mass Spectrometry of Nucleosides. Mechanisms of Ion Formation and Estimations of Proton Affinity. *J. Am. Soc. Mass Spectrom.* **1975,** *97,* 3436–3444.
16. Liguori, A.; Napoli, A.; Sindona, G. Determination of Substituent Effects on the Proton Affinities of Natural Nucleosides by the Kinetic Method. *Rapid Commun. Mass Spectrom.* **1994,** *8,* 89–93.
17. Frisch, M. J.; Trucks, G. W.; Schlegel, H. B.; Scuseria, G. E.; Robb, M. A.; Cheeseman, J. R.; Montgomery, J. A., Jr.; Vreven, T.; Kudin, K. N.; Burant, J. C.; Millam, J. M.; Iyengar, S. S.; Tomasi, J.; Barone, V.; Mennucci, B.; Cossi, M.; Scalmani, G.; Rega, N.; Petersson, G. A.; Nakatsuji, H.; Hada, M.; Ehara, M.; Toyota, K.; Fukuda, R.; Hasegawa, J.; Ishida, M.; Nakajima, T.; Honda, Y.; Kitao, O.; Nakai, H.; Klene, M.; Li, X.; Knox, J. E.; Hratchian, H. P.; Cross, J. B.; Adamo, C.; Jaramillo, J.; Gomperts, R.; Stratmann, R. E.; Yazyev, O.; Austin, A. J.; Ammi, R.; Pomelli, C.; Ochterski, J. W.; Ayala, P. Y.; Morokuma, K.; Voth, G. A.; Salvador, P.; Dannenberg, J. J.; Zakrzewski, V. G.; Dapprich, S.; Daniels, A. D.; Strain, M. C.; Farkas, O.; Malick, D. K.; Rabuck, A. D.; Raghavachari, K.; Foresman, J. B.; Ortiz, J. V.; Cui, Q.; Baboul, A. G.; Clifford, S.; Cioslowski, J.; Stefanov, B. B.; Liu, G.; Liashenko, A.; Piskorz, P.; Komaromi, I.; Martin, R. L.; Fox, D. J.; Keith, T.; Al-Laham, M. A.; Peng, C. Y.; Nanayakkara, A.; Hallacombe, M.; Gill, P. M. W.; Johnson, B.; Chen, W.; Wong, M. W.; Gonzalez, C.; Pople, J. A. *Gaussian 03*, revision B. 01; Gaussian, Inc.: Wallingford CT, 2004.
18. Hocquet, A.; Leulliot, N.; Ghomi, M. Ground-State Properties of Nucleic Acid Constituents Studied by Density Functional Calculations. 3. Role of Sugar Puckering and Base Orientation on the Energetics and Geometry of 2′-Deoxyribonucleosides and Ribonucleosides. *J. Phys. Chem. B* **2000,** *104,* 4560–4568.
19. Huang, Y.; Kenttamaa, H. Theoretical Estimations of the 298 K Gas-Phase Acidities of the Purine-Based Nucleobases Adenine and Guanine. *J. Phys. Chem. A* **2004,** *108,* 4485–4490.
20. Drahos, L.; Vekey, K. Entropy Evaluation Using the Kinetic Method: is it Feasible? *J. Mass Spectrom.* **2003,** *38,* 1025–1042.
21. Cooks, R. G.; Patrick, J. S.; Kotiaho, T.; McLuckey, S. A. Thermochemical Determinations by the Kinetic Method. *Mass Spectrom. Rev.* **1994,** *13,* 287–339.
22. Mc Luckey, S. A.; Cameron, D.; Cooks, R. G. Proton Affinities from Dissociations of Proton-Bound Dimers. *J. Am. Chem. Soc.* **1981,** *103,* 1313–1317.
23. Ervin, K. M.; Armentrout, P. B. Systematic and Random Errors in Ion Affinities and Activation Entropies from the Extended Kinetic Method. *J. Mass Spectrom.* **2004,** *39,* 1004–1015.
24. Drahos, L.; Peltz, C.; Vekey, K. Accuracy of Enthalpy and Entropy Determination Using the Kinetic Method: Are We Approaching a Consensus? *J. Mass Spectrom.* **2004,** *39,* 1016–1024.
25. Bouchoux, G. Microcanonical Modeling of the Thermokinetic Method. *J. Phys. Chem. A* **2006,** *110,* 8259–8265.
26. Bouchoux, G.; Sablier, M.; Berruyer-Penaud, F. Obtaining Thermochemical Data by the Extended Kinetic Method. *J. Mass Spectrom.* **2004,** *39,* 986–997.
27. Wesdemiotis, C. Entropy Considerations in Kinetic Method Experiments. *J. Mass Spectrom.* **2004,** *39,* 998–1003.
28. Ervin, K. M. Microcanonical Analysis of the Kinetic Method. The Meaning of the "Apparent Entropy." *J. Am. Soc. Mass Spectrom.* **2002,** *13,* 435–452.
29. Ravi Kumar, M.; Prabhakar, S.; Nagaveni, V.; Vairamani, M. Estimation of Gas-Pphase Acidities of a Series of Dicarboxylic Acids by the Kinetic Method. *Rapid Commun. Mass Spectrom.* **2005,** *19,* 1053–1057.
30. Armentrout, P. B. Entropy Measurements and the Kinetic Method: A Statistically Meaningful Approach. *J. Am. Soc. Mass Spectrom.* **2000,** *11,* 371–379.
31. Caldwell, G. W.; Masucci, J. A.; Ikonomous, M. G. Negative Ion Chemical Ionization Mass Spectrometry-Binding of Molecules to Bromide and Iodide Anions. *Org. Mass Spectrom.* **1989,** *24,* 8–14.

32. Linstrom, P. J.; Mallard, W. G., Eds.; *NIST Chemistry Webbook, NIST Standard Reference Database Number 69, June 2005 Release*; National Institute of Standards and Technology: Gaithersburg, MD (http://webbook.nist.gov).
33. Corfu, N. A.; Sigel, H. Acid-Base Properties of Nucleosides and Nucleotides as a Function of Concentration. Eur. J. Biochem. **1991,** *199*, 659–669.
34. Tribolet, R.; Sigel, H. Self-Association and Protonation of Adenosine 5′-Monophosphate in Comparison with its 2′- and 3′-Analogues and Tubercidin 5′-Monophosphate (7-deaza-AMP), *Eur. J. Biochem.* **1987,** *163,* 353–363.
35. Mucha, A.; Knobloch, B.; Jezówska-Bojczuk, M.; Kozłowski, H.; Sigel, R. K. O. Comparison of the Acid-Base Properties of Ribose and 2′-Deoxyribose Nucleotides. *Chem. Eur. J.* **2008,** *14,* 6663–6671.
36. Topol, A.; Burt, S. K.; Russo, N.; Toscano, M. Theoretical Calculations of Glycine and Alanine Gas-Phase Acidities. *J. Am. Soc. Mass Spectrom.* **1999,** *10,* 318–322.
37. Huang, Y.; Kenttamaa, H. Theoretical Estimations of the 298 K Gas-Phase Acidities of the Pyrimidine-Based Nucleobases Uracil, Thymine, and Cytosine. *J. Phys. Chem. A* **2003,** *107,* 4893–4897.